# X-ray Diffraction and X-ray Absorption Spectroscopy Studies of Sol−Gel-Processed Zirconium Titanates

J. Xu, C. Lind, A. P. Wilkinson,* and S. Pattanaik†

*School of Chemistry & Biochemistry, Georgia Institute of Technology, Atlanta, Georgia 30332-0400*

*Received April 11, 2000. Revised Manuscript Received August 8, 2000*

$ZrTiO_4$ samples were prepared by using a conventional hydrolytic alkoxide sol−gel route, a nonhydrolytic method, an acetic acid modified route, and by the direct reaction of the binary oxides. The local structure in the gels and its evolution upon heating was followed using EXAFS and XANES, and the crystallization of the products was examined using powder X-ray diffraction. All the solution-processed materials crystallized in the range 600−700 °C. The crystalline materials formed at 700 °C showed no evidence of any long-range cation ordering. The EXAFS data indicated that all the amorphous $ZrTiO_4$ samples produced using the solution routes contained zirconium with a coordination number >6 and that the disordered crystalline $ZrTiO_4$ contained six-coordinate zirconium. Both the XANES and EXAFS data showed that nearly all the amorphous $ZrTiO_4$ samples contained titanium with a coordination number of <6. The EXAFS data clearly indicated the presence of Zr−O−Ti links in the $ZrTiO_4$ gel produced using the nonhydrolytic route. There was also some evidence that the gel prepared using hydrolytic sol−gel chemistry contained Zr−O−Ti links.

## Introduction

Zirconium-titanate- (ZT-) based materials are widely used in electrical applications where low-cost, temperature-stable dielectrics are required.[1] The composition $Zr_{0.8}Sn_{0.2}TiO_4$ is of particular technological significance as it has a high dielectric constant ($K = 35$) and a large $Q$ value at high frequencies ($Q = 6800$ at 6 GHz).[2] It has been used as a resonator material since 1970. The technological applications of zirconium titanates have led to considerable interest in their crystal structures, phase transformations, and processing.

The $ZrO_2$−$TiO_2$ phase diagram has been investigated by McHale and Roth.[3] Above 1100 °C there exists a stable solid solution, $Zr_{1+x}Ti_{1-x}O_4$, with approximate limits $-0.17 < x < 0.1$ ($x \sim -0.17$ corresponds to $Zr_5Ti_7O_{24}$). At lower temperatures $ZrTiO_4$ is not thermodynamically stable, but a solid solution centered around the composition $ZrTi_2O_6$ is stable. However, a wide range of compositions in the solid solution $Zr_{1+x}Ti_{1-x}O_4$ can be obtained in metastable form either by wet chemical methods (35−75 mol % Ti) or by quenching from high temperatures as the decomposition kinetics are very slow.[3]

The structure of $ZrTiO_4$ was first investigated in 1967. It was reported to be a close structural relative of columbite, $(Fe,Mn)Nb_2O_6$,[4] a compound that has an $\alpha$-$PbO_2$ substructure. This early work examined the disordered high-temperature form of $ZrTiO_4$, which only contains metal ions in six-coordinated sites. There exists an order−disorder transformation at around 1125 °C[3] that only occurs to a significant extent upon slow cooling. Electron diffraction has shown that the ordered low-temperature phase is related to the $\alpha$-$PbO_2$ structure by a commensurate 2× superstructure.[1] A bulk sample of $ZrTiO_4$ showing a commensurate superlattice has, as far as we are aware, never been fully structurally characterized. However, a neutron diffraction study of ordered $Zr_5Ti_7O_{24}$ has been carried out.[5] This compound has an $AB_2O_6$ structure related to that of $\alpha$-$PbO_2$ by a 3× increase in the *a*-axis length and distortions that lead to the presence of both eight- (A sites) and six- (B sites) coordinated cations. The $Zr_5Ti_7O_{24}$ stoichiometry is accommodated within this structure by an imperfect ordering of the Zr and Ti between the A and B sites. The room-temperature lattice parameters for $ZrTiO_4$ are dependent upon the degree of cation ordering in the material. The order−disorder transformation is a complex process that is strongly dependent upon the presence of dopants as well as thermal history. Yttrium doping enhances the ordering process whereas tin suppresses it.[2,6]

$ZrTiO_4$ can be prepared by the reaction of $ZrO_2$ and $TiO_2$ at ∼1350 °C. However, this can lead to inhomogeneous, coarse, and multiphase powders of poor purity. Therefore, alternative approaches to the preparation of high-quality powders have been explored. The routes investigated include a polymeric precursor made from titanium butoxide and zirconium oxychloride octahydrate,[7,8] coprecipitation from aqueous solution,[9−11] elec-

* To whom correspondence should be addressed.
† Current address: The Consortium for Fuel Liquefaction Science, University of Kentucky, Room 111, 533 South Limestone Street, Lexington, KY 40506-0043.

(1) Christoffersen, R.; Davies, P. K. *J. Am. Ceram. Soc.* **1992**, *75*, 563−569.
(2) Christofferson, R.; Davis, P. K.; Wei, X. *J. Am. Ceram. Soc.* **1994**, *77*, 1441−50.
(3) McHale, A.; Roth, R. *J. Am. Ceram. Soc.* **1986**, *69*, 827−32.
(4) Newnham, R. E. *J. Am. Ceram. Soc.* **1967**, *50*, 216.
(5) Bordet, P.; McHale, A.; Santoro, A.; Roth, R. S. *J. Solid State Chem.* **1986**, *64*, 30−46.
(6) Park, Y. *Solid State Commun.* **1999**, *109*, 489−493.
(7) Bianco, A.; Gusmano, G.; Freer, R.; Smith, P. *J. Eur. Ceram. Soc.* **1999**, *19*, 959−963.

10.1021/cm000298s CCC: $19.00 
Published on Web 11/02/2000

trolytic deposition,[12] mechanochemical synthesis,[13] conventional alkoxide sol−gel methods,[3,14] a nonalkoxide sol−gel procedure in which zirconium acetylacetonate was mixed with acetic-acid-modified titanium isopropoxide,[15] and nonhydrolytic sol−gel routes.[16]

In this paper, four procedures for the preparation of $ZrTiO_4$ are compared: a conventional alkoxide sol−gel route, an acetic-acid-modified sol−gel route based on that previously reported for lead zirconium titanate (PZT),[17,18] a nonhydrolytic sol−gel method, and a mixed oxide route. Powder X-ray diffraction and EXAFS (extended X-ray absorption fine structure) were employed to study the effect of processing chemistry on both the crystallization and local structures of the materials. This work is an extension of our experiments on other solution-processed zirconium- and titanium-containing ceramics.[19]

There have been several X-ray absorption spectroscopy (XAS) studies of the local structures around zirconium and titanium in solution-processed high dielectric constant materials such as PZT[20−28] and calcium zirconium titanate (CZT).[19] However, there has been very little work on pure zirconium titanates. Bertagnolli's group has reported an EXAFS study of mixed zirconium and titanium alkoxides,[29] and McHale et al.[30] have investigated $Zr_{0.8}Sn_{0.2}TiO_4$ using EXAFS.

## Experimental Section

**Syntheses.** Stock solutions of zirconium butoxide (97%, Aldrich) and titanium isopropoxide (80%, Aldrich) in 2-methoxyethanol were used as starting materials for all the hydrolytic sol−gel experiments. Their concentrations were determined gravimetrically to be 0.717 and 1.402 M, respectively. All the $ZrTiO_4$ samples were slow-cooled either inside the furnace or on a piece of firebrick outside the furnace after heat treatment.

*Alkoxide Sol−Gel Method*. Stoichiometric amounts of zirconium and titanium stock solutions were mixed and refluxed for 1 h. The flask was opened to air for 4 days. The resulting gel was vacuum-dried overnight at 110 °C. Portions of dry gel were heated at 5 °C/min to 600, 700, 800, and 1000 °C and held at these temperatures for 5 h. A similar approach was employed to prepare both $TiO_2$ and $ZrO_2$ powders.

*Acetic-Acid-Modified Route*. Zirconium butoxide (4.57 mL, as purchased) was mixed with 3.07 mL of titanium isopropoxide (as purchased); 4.81 mL of acetic acid was added to the mixture after 5 min. Then, 10 mL of methanol was added after another 5 min. The solution was stirred during the whole procedure. Volatiles were removed at 75 °C under vacuum. The residual solid was then heated under vacuum overnight at 110 °C to obtain a dry gel. Portions of the dry gel were heated at 5 °C/min to 600, 700, 800, 900, and 1000 °C and held there for 5 h.

*Mixed Oxide Method*. Predried $ZrO_2$ and $TiO_2$ were used as starting materials. The reactants were ball-milled in ethanol for 1 h and heated to 1400 °C for 5 h.

*Nonhydrolytic Sol−Gel Method*. As the starting materials used for these syntheses react readily with water, care was taken to avoid contact with moisture. All the steps prior to breaking the tubes at the end of the reaction were carried out using dry reagents under argon. The addition of $(i\text{Pr})_2O$ to the starting materials was carried out while cooling in an ice bath as the reaction is exothermic. The tubes were cooled in liquid nitrogen, evacuated, and sealed prior to heating at the reaction temperature. The samples were recovered by breaking the tubes under an inert atmosphere, suspending in ∼100 mL of $CHCl_3$ and separating using a centrifuge. The powders were then dried under vacuum at room temperature (dry gels).

*$ZrO_2$*. $ZrCl_4$ (5.67 g, 24 mmol) was suspended in 7 mL of $CHCl_3$ in a glass tube; 14 mL of $(i\text{Pr})_2O$ (99 mmol) was added slowly. The mixture was then stirred for ≈30 min at room temperature. During this time, gelation started. The evacuated sealed tube was heated at 110 °C for 7 days. A white powder was recovered. The resulting dry gel was heated to 200 °C at 5°/min and held for 2 h. Additional samples were obtained by heating portions of this material at 5°/min to 300, 400, 450, 500, and 600 °C for 1−4 h.

*$TiO_2$*. $TiCl_4$ (7.1 g, 37.5 mmol) was suspended in 5.5 mL of $CHCl_3$; 10.5 mL of $(i\text{Pr})_2O$ (75 mmol) was added rapidly while stirring. A pale yellow gel formed within 2 min. The sealed evacuated tube was heated to 70 °C for 7 days. A white powder was recovered. Additional samples were obtained by heating portions of the dry gel at 5°/min to 200 °C for 2 h, 250 °C for 4 h, 300 °C for 2 h, and 500 °C for 1 h.

*$ZrTiO_4$*. A mixture of 3.44 g of $ZrCl_4$ (14.8 mmol) and 2.8 g of $TiCl_4$ (14.8 mmol) was suspended in 4.3 mL of $CHCl_3$; 8.5 mL of $(i\text{Pr})_2O$ (60.3 mmol) was added slowly while stirring. The mixture was stirred for ≈30 min at room temperature. The sealed evacuated tube was heated to 110 °C for 7 days. A brown powder was recovered (NHDG). An amorphous sample (NH600) was prepared by heating some dry gel to 600 °C at 5°/min and holding for 45 min. Crystalline materials were obtained by (i) heating a sample at 5 °C/min to 700 °C for 1 h (NH700) and (ii) placing a sample in a preheated furnance at 1200 °C for 20 min (NH1200).

**Characterization.** *Powder X-ray Diffraction*. All data were collected using a Scintag X1 powder instrument equipped with a Scintag Peltier cooled solid-state detector and employing Cu Kα radiation.

(8) Bianco, A.; Paci, M.; Freer, R. *J. Eur. Ceram. Soc.* **1998**, *18*, 1235−1243.
(9) Bhattacharya, A. K.; Mallick, K. K.; Hartridge, A.; Woodhead, J. L. *J. Mater. Sci.* **1996**, *31*, 267−271.
(10) Bhattacharya, A. K.; Hartridge, A.; Mallick, K. K.; Taylor, D. *J. Mater. Sci.* **1996**, *31*, 5583−5586.
(11) Navio, J. A.; Marchena, F. J.; Macias, M.; Sanchez-Soto, P. J. *J. Mater. Sci.* **1992**, *27*, 2463−2467.
(12) Zhitomirsky, I.; Gal-or, L.; Klein, S. *J. Mater. Sci. Lett.* **1995**, *14*, 60−62.
(13) Isobe, T.; Okamoto, Y.; Senna, M. *Mater. Res. Soc. Proc.* **1994**, *346*, 273−277.
(14) Yamaguchi, O.; Mogi, H. *J. Am. Ceram. Soc* **1989**, *72*, 1065−1066.
(15) Khairulla, F.; Phule, P. *Mater. Sci. Eng.* **1992**, *B12*, 327−336.
(16) Andrianainarivelo, M.; Corriu, R. J. P.; Leclercq, D.; Mutin, P. H.; Vioux, A. *J. Mater. Chem.* **1997**, *7*, 279−284.
(17) Assink, R. A.; Schwartz, R. W. *Chem. Mater.* **1993**, *5*, 511−517.
(18) Schwartz, R. W.; Assink, R. A.; Dimos, D.; Sinclair, M. B.; Boyle, T. J.; Buchheit, C. D. *Mater. Res. Symp. Proc.* **1995**, *361*, 377−387.
(19) Xu, J.; Wilkinson, A. P.; Pattanaik, S. *Chem. Mater.*, in press.
(20) Kolb, U.; Gutwerk, D.; Beudert, R.; Bertagnolli, H. *J. Non-Cryst. Solids* **1997**, *217*, 162−166.
(21) Peter, D.; Ertel, T. S.; Bertagnolli, H. *J. Sol-Gel Sci. Technol.* **1995**, *5*, 5−14.
(22) Ahlfanger, R.; Bertagnolli, H.; Ertel, T.; Kolb, U.; Peter, D.; Nass, R.; Schmidt, H. *Ber. Bunsen-Ges. Phys. Chem.* **1991**, *95*, 1286−1289.
(23) Kolb, U.; Gutwaerk, D.; Beudert, R.; Ertel, T. S.; Abraham, I.; Horner, W.; Bertagnolli, H. *EXAFS: Structure Investigations on PZT Precursors*; Daresbury Laboratory: United Kingdom, 1995.
(24) Kolb, U.; Abraham, I.; Gutwerk, D.; Ertel, T. S.; Horner, W.; Bertagnolli, H.; Merklein, S.; Sporn, D. *Physica B* **1995**, *208/209*, 601−603.
(25) Antonioli, G.; Bersani, D.; Lottici, P. P.; Manzini, I.; Bassi, S.; Gnappi, G.; Montenero, A. *J. Phys. IV (Paris)* **1997**, *7*, C2−1161.
(26) Malic, B.; Arcon, I.; Kosec, M.; Kodre, A. *J. Sol-Gel Sci. Technol.* **1997**, *8*, 343−346.
(27) Sengupta, S. S.; Ma, L.; Adler, D. L.; Payne, D. A. *J. Mater. Res.* **1995**, *10*, 1345−1348.
(28) Malic, B.; Arcon, I.; Kosec, M.; Kodre, A. *J. Mater. Res.* **1997**, *12*, 2602−2611.
(29) Reinohl, U.; Ertel, T. S.; Horner, W.; Weber, A.; Bertagnolli, H. *Ber. Bunsen-Ges. Phys. Chem.* **1998**, *102*, 144−147.
(30) Kudesia, R.; Snyder, R. L.; Condrate, R. A.; McHale, A. E. *J. Phys. Chem. Solids* **1993**, *54*, 671−684.

**Table 1. Samples Examined by EXAFS and $\Delta k$ (Å$^{-1}$) Available for Analysis**

| sample code | sample | synthesis procedure[a] | Ti K-edge $\Delta k$ (Å$^{-1}$) | Zr K-edge $\Delta k$ (Å$^{-1}$) | data collection location |
|---|---|---|---|---|---|
| HDG | $ZrTiO_4$ | HSG, dry gel | 1−15.20 | 1−16.00 | NSLS |
| H600 | $ZrTiO_4$ | HSG, 600 °C, 5 h | 1−16.10 | 1−14.50 | NSLS |
| H700 | $ZrTiO_4$ | HSG, 700 °C, 5 h | 1−15.00 | 1−16.80 | NSLS |
| ADG | $ZrTiO_4$ | AA, dry gel | 1−15.00 | 1−14.50 | NSLS |
| A600 | $ZrTiO_4$ | AA, 600 °C, 5 h | 1−14.30 | 1−13.90 | NSLS |
| A700 | $ZrTiO_4$ | AA, 700 °C, 5 h | 1−15.20 | 1−16.33 | NSLS |
| NHDG | $ZrTiO_4$ | NHSG, dry gel | 1−15.20 | 1−16.49 | $^{Ti}$NSLS, $^{Zr}$SSRL |
| NH600 | $ZrTiO_4$ | NHSG, 600 °C | 1−15.20 | 1−16.49 | $^{Ti}$NSLS, $^{Zr}$SSRL |
| NH700 | $ZrTiO_4$ | NHSG, 700 °C | 1−15.20 | 1−16.80 | $^{Ti}$NSLS, $^{Zr}$SSRL |
| NH1200 | $ZrTiO_4$ | NHSG, 1200 °C | N/A | 1−16.50 | $^{Ti}$NSLS, $^{Zr}$SSRL |
| C1400 | $ZrTiO_4$ | MO, 1400 °C, 5 h | N/A | 1−16.06 | NSLS |
| ZHSG | $ZrO_2$ | HSG, dry gel | N/A | 0.35−17.00 | NSLS |
| Z1000 | $ZrO_2$ | HSG, 1000 °C | N/A | 1−17.40 | NSLS |
| ZNHDG | $ZrO_2$ | NHSG, dry gel | N/A | 1−15.00 | SSRL |
| ZNH200 | $ZrO_2$ | NHSG, 200 °C | N/A | 1−16.46 | SSRL |
| ZNH600 | $ZrO_2$ | NHSG, 600 °C | N/A | 1−16.46 | SSRL |
| ZREF | $ZrO_2$ | monoclinic | N/A | 1−17.95 | SSRL |
| TNHDG | $TiO_2$ | NHSG, dry gel | 2.62−13.14 | N/A | SSRL |
| TNH500 | $TiO_2$ | NHSG, 500 °C | 2−15.00 | N/A | SSRL |
| T1000 | $TiO_2$ | sol−gel, 1000 °C, 5 h | 1−15.20 | N/A | NSLS |

[a] HSG = homogeneous sol−gel; AA = acetic-acid-modified sol−gel; NHSG = nonhydrolytic sol−gel; MO = mixed oxide; N/A = not applicable.

*X-ray Absorption Spectroscopy Data Collection*. Zr and Ti K-edge transmission XAS spectra were measured at room temperature using either beam line X11A at National Synchrotron Light Source (NSLS) or beam line 2−3 at the Stanford Synchrotron Radiation Laboratory (SSRL). Only the nonhydrolytic sol−gel samples were examined at SSRL. A Si(111) double-crystal monochromator was employed for all the measurements along with a beam size of $10 \times 1$ mm$^2$ for the experiments at the NSLS and $15 \times 2$ mm$^2$ for the experiments at the SSRL. All the spectra were obtained using a three ion-chamber arrangement with the sample between the first two detectors and a reference foil between the second and third detectors. A summary of the data collected and the naming scheme for the samples is presented in Table 1.

*EXAFS Data Analysis*. The XAS data analyses were performed using the program package EXAFSPAK.[31] Phase and amplitude functions were calculated using the program FEFF7.[32]

## Results and Discussion

**Powder Diffraction Studies.** Powder diffraction data for the heat-treated $ZrTiO_4$ (ZT) samples prepared by the homogeneous sol−gel (HSG) route, acetic-acid-modified sol−gel (AAM) route, and the nonhydrolytic sol−gel (NHSG) route are shown in Figure 1. The crystallization behavior is broadly independent of the synthetic method employed. In every case the crystallization of $ZrTiO_4$ occurred between 600 and 700 °C. This is typical of solution-processed $ZrTiO_4$; see for example a recent paper on alkoxide sol−gel-processed ZT,[33] although temperatures down to ≈440 °C have been reported.[34]

The lattice constants for all the crystalline samples are available as Supporting Information. They vary in the ranges $a = 4.780-4.811$, $b = 5.439-5.516$, and $c = 5.025-5.033$ Å. It is notable that the variation in $b$ is large and that it has been reported to depend on the extent of the cation ordering in $ZrTiO_4$.[3] Completely disordered materials prepared by quenching from temperatures around 1400 °C have $b$ axis lengths of ≈5.50 Å whereas ordered materials prepared by annealing at <1100 °C have $b$ axis lengths of 5.36 Å.[3] Our lattice constants for the crystalline $ZrTiO_4$ samples prepared at 700 °C indicate that they are fully disordered materials.[2] This is not the thermodynamically most stable cation arrangement at low temperatures, but the disorder that is present in the initial amorphous materials is presumably carried over into the crystalline product. Partial ordering occurs in some of the samples heat-treated at higher temperatures, presumably because of the slow cooling that was employed. No superlattice peaks indicative of long-range cation ordering were observed for any of the crystalline $ZrTiO_4$ samples. While Yamaguchi has reported[14] the preparation of partially ordered $ZrTiO_4$ samples using alkoxide sol−gel chemistry and a ≈700 °C heat treatment, the formation of disordered $ZrTiO_4$ at 700 °C has previously been observed for samples prepared using both alkoxide sol−gel[35] and coprecipitation[36] methods.

The heat-treated $ZrO_2$ gel processed by the nonhydrolytic sol−gel route started to show some signs of crystallization at 300−400 °C, and at 450 °C the powder pattern was consistent with the presence of some poorly crystalline tetragonal or cubic zirconia. At 600 °C a mixture of cubic/tetragonal and a small amount of monoclinic $ZrO_2$ had formed. The $TiO_2$ dry gel processed by the nonhydrolytic sol−gel route initially crystallized with the anatase structure at ≈250 °C. It is notable that both $ZrO_2$ and $TiO_2$ crystallized at a lower temperature than the $ZrTiO_4$ prepared using the same method.

The $ZrO_2$ dry gel prepared by the alkoxide sol−gel route crystallized into a mixture of tetragonal/cubic $ZrO_2$ and monoclinic $ZrO_2$ at ≈500 °C. As the heat treatment

(31) George, G. N.; Pickering, I. J. *EXAFSPAK A Suite of Programs for Analysis of X-ray Absorption Spectra*.
(32) Zabinsky, S. I.; Rehr, J. J.; Ankubinov, A.; Albers, R. C.; Eller, M. J. *Phys. Rev. B* **1995**, *52*, 2995.
(33) Sham, E. L.; Aranda, M. A. G.; Farfan-Torres, E. M.; Gottifredi, J. C.; Martinez-Lara, M.; Bruque, S. *J. Solid State Chem.* **1998**, *139*, 225−232.
(34) Bhattacharya, A. K.; Mallick, K. K.; Hartridge, A.; Woodhead, J. L. *Mater. Lett.* **1994**, *18*, 247.
(35) Xu, Q.; Anderson, M. A. *J. Am. Ceram. Soc.* **1993**, *76*, 2093−97.
(36) Daturi, M.; Cremona, A.; Milella, F.; Busca, G.; Vogna, E. *J. Eur. Ceram. Soc.* **1998**, *18*, 1079−1087.

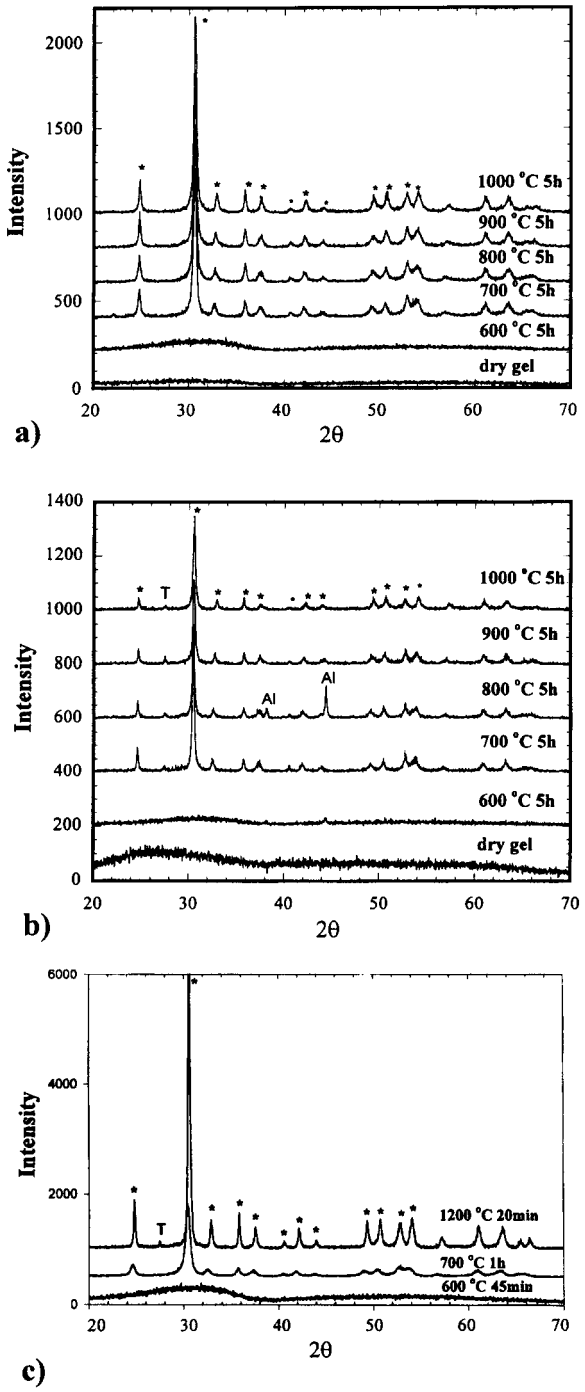


**Figure 1.** Powder X-ray diffraction patterns for the heat-treated $ZrTiO_4$ samples: (a) prepared using the alkoxide sol−gel (HSG) method, (b) prepared using the acetic-acid-modified sol−gel (AAM) method, and (c) prepared using the nonhydrolytic sol−gel (NHSG) method. *, $ZrTiO_4$; T, rutile $TiO_2$; Al, peaks from an aluminum sample holder.

temperature increased, the tetragonal/cubic $ZrO_2$ transformed to monoclinic $ZrO_2$. Almost pure monoclinic $ZrO_2$ was obtained after 5 h at 1000 °C. The $TiO_2$ prepared using alkoxide sol−gel chemistry crystallized as anatase at 500 °C. A mixture of rutile and anatase was obtained at 600 °C. Pure rutile was obtained at 700 °C.

**Titanium XANES Experiments.** The Ti K-edge XANES spectra of all the samples are compared with one another in Figure 2. Two distinct types of spectra are observed. Many of the samples display a single relatively high intensity pre-edge feature, while the

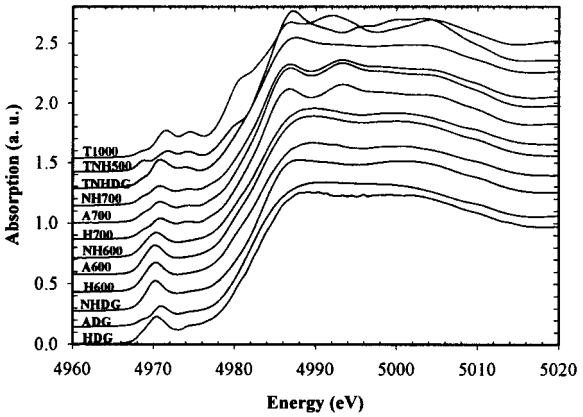


**Figure 2.** Ti K-edge XANES for the $ZrTiO_4$ and $TiO_2$ samples. They can be divided into two categories, those with a single strong pre-edge peak and those with multiple weaker peaks. The single pre-edge peak at ≈4970 eV suggests the presence of five-coordinated titanium.[39]

others show three pre-edge peaks with relatively low intensities. It is notable that the amorphous samples, with the exception of the $ZrTiO_4$ dry gel prepared by the acetic-acid-modified method (sample ADG) and the $TiO_2$ dry gel prepared by the nonhydrolytic route (sample TNHDG), show a single pre-edge peak.

The Ti pre-edge features are attributable to transitions from Ti 1s to Ti 3d orbitals. Different Ti coordination environments can be identified using the Ti K-edge XANES. Farges et al.[37−44] showed that $^4$Ti, $^5$Ti, and $^6$Ti (four-, five-, and six-coordinate titanium) are distinguishable according to the positions and heights of the pre-edge peaks. However, there is some variation in the XANES spectra for compounds containing $^6$Ti. Materials with distorted and regular octahedra show lower and higher pre-edge peak energies, respectively.

Our pre-edge data were normalized and then fit over the energy range 4960−4980 eV using pseudo-Voigt peaks for each of the pre-edge features and a step function for the edge jump. The peak positions, normalized heights, and half-widths for the major peaks in each of the spectra are available as Supporting Information. As the peak heights are sensitive to the experimental conditions employed, both peak heights and peak positions were used in a comparison with the literature values for well-characterized titanium compounds. The main peak positions for our rutile (T1000), anatase (TNH500), and crystalline $ZrTiO_4$ samples were all shifted to lower energy by 0.2 eV when compared to the work of Farges et al.[37−44] This was taken into account when comparing the peak positions for our unknowns with the literature data.

The major peak in the XANES spectra of all the crystalline $ZrTiO_4$ samples (H700, A700, and NH700)

(37) Farges, F. *J. Non-Cryst. Solids* **1996**, *204*, 53−64.
(38) Farges, F.; Brown, G. B.; Rehr, J. J. *Geochim. Cosmochim. Acta* **1996**, *60*, 3023−3038.
(39) Farges, F.; Brown, G. E.; Navrotsky, A.; Gan, H.; Rehr, J. J. *Geochim. Cosmochim. Acta* **1996**, *60*, 3039−3053.
(40) Farges, F.; Brown, G. E.; Rehr, J. J. *Phys. Rev. B* **1997**, *56*, 1809−1819.
(41) Farges, F. *Am. Miner.* **1997**, *82*, 44−50.
(42) Farges, F.; Brown, G. B. *Geochim. Cosmochim. Acta* **1997**, *61*, 1863−1870.
(43) Farges, F.; Brown, G. B.; Rehr, J. J. *J. Phys. IV (Paris)* **1997**, *7*, C2 191−193.
(44) Farges, F. *Am. Miner.* **1997**, *82*, 36−43.

is shifted to higher energy by ≈0.5 eV and has a lower peak intensity when compared to the major peak in the XANES spectra of the amorphous samples (HDG, H600, A600, NHDG, and NH600). Because of the distorted octahedra in crystalline $ZrTiO_4$, the pre-edge peak for this compound is expected to be shifted to higher energy by ≈0.5 eV relative to that for a material containing five-coordinated titanium.[40] The qualitative appearance of our XANES spectra and the fitting of the pre-edge data are both consistent with the presence of five-coordinated titanium in all of the amorphous materials, with the exception of the ADG and TNHDG samples. This is in agreement with our previous study of amorphous $Ca(Zr_xTi_{1-x})O_3$,[19] samples that were prepared by alkoxide sol−gel methods.

It is interesting to note that although the amorphous ADG sample displayed three pre-edge peaks whose positions and heights were similar to those for the crystalline $ZrTiO_4$ samples, suggesting that the titanium is in an octahedral environment, the XANES data for the A600 sample are consistent with the presence of five-coordinated titanium. This indicates a reduction in coordination number as the residual organics are burnt out of the sample. The pre-edge features for the $TiO_2$ dry gel prepared by nonhydrolytic sol−gel chemistry (TNHDG) differ from those observed for crystalline anatase (TNH500) and rutile (T1000) and from that expected for pure five-coordinated titanium. However, they occur at the same energy as the peaks for crystalline $ZrTiO_4$ but with considerably higher intensity. This is consistent with the presence of both five- and six-coordinated titanium in the TNHDG sample.[38]

**Ti K-Edge EXAFS Studies.** *Titanium Oxide Samples.* Because of the disordered nature of the $TiO_2$ dry gel sample (TNHDG) and the limited data range that was available for analysis ($k_{max} \sim 13.74$ Å$^{-1}$), there was only one well-defined peak, at ≈1.5 Å, in the FT magnitude for this sample. It can be attributed to backscattering from oxygen. This peak was transformed into *k*-space and several models for the EXAFS were explored. The $E_0$ value used for these analyses was obtained by fitting our anatase/rutile data using their known crystal structures. An octahedral model based on the crystal structures of rutile and anatase gave a poor fit to the data for the TNHDG sample. However, a single-shell model in which the coordination number, interatomic distance, and the Debye−Waller factor were refined simultaneously gave a reasonable fit with a metal−oxygen distance of ≈1.91 Å. This is considerably shorter than that expected for six-coordinated titanium (≈1.96 Å) and suggests that there is some titanium in the sample with a coordination number of <6. This is consistent with the observed pre-edge spectrum.

*Zirconate Titanate Samples.* The Ti K-edge FT magnitudes for the $ZrTiO_4$ samples are shown in Figure 3. In the oxygen backscattering region, the FT magnitudes are independent of the processing chemistry employed for the dry gel and 600 °C samples. The differences observed in the oxygen backscattering region for the 700 °C samples are almost certainly artifacts of the data processing procedures that were employed. The low *R* regions of the FTs are most sensitive to problems of this type. All the FT magnitudes for the crystalline samples (H700, A700, and NH700—Figure 3c) are similar to one another in the metal backscattering region, and those for the amorphous materials resulting from a 600 °C heat treatment (H600, A600, and NH600—Figure 3b) are also quite similar to one another. However, the spectra for the dry gel samples (Figure 3a) are quite different from one another in the region where metal backscattering is expected. This suggests that the choice of processing chemistry has the most profound effect on the local structure in the dry gels and that differences in the metal shell diminish as the heat treatment temperature increases. The differences that were present

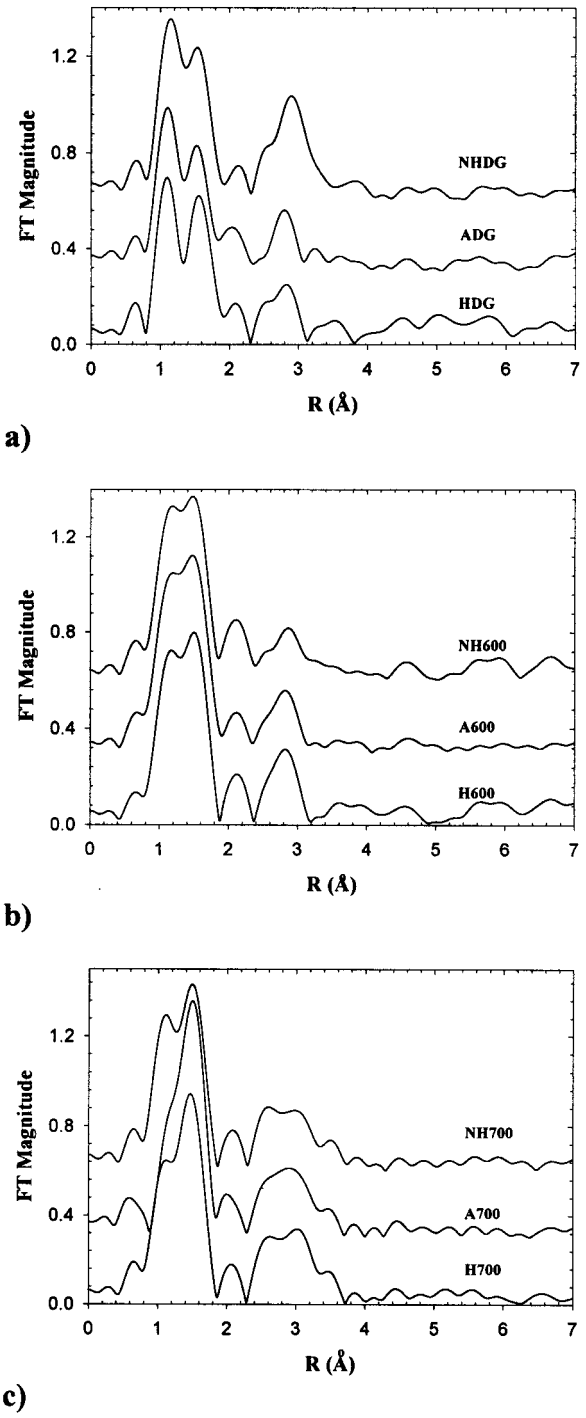


**Figure 3.** Ti K-edge Fourier transform magnitudes for all the $ZrTiO_4$ (a) dry gels, (b) samples heat-treated at 600 °C, and (c) samples heat-treated at 700 °C. Only the samples heated to 700 °C were crystalline. The Fourier transforms were carried out over the range 1−14 Å$^{-1}$.

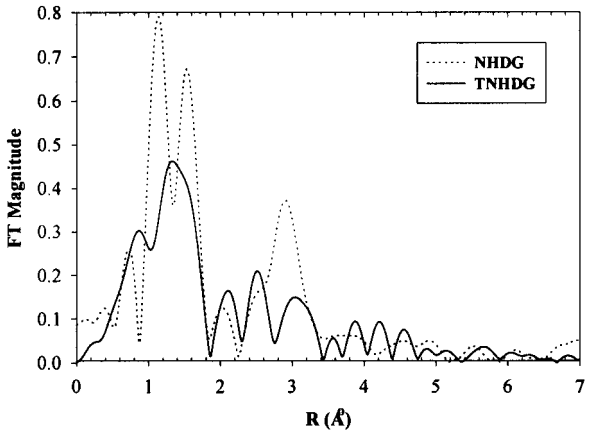


**Figure 4.** Ti K-edge Fourier transform magnitudes for the TNHDG ($TiO_2$ dry gel) and NHDG ($ZrTiO_4$ dry gel) samples. Both materials were prepared using nonhydrolytic sol−gel chemistry under similar conditions. The pronounced difference between the Fourier transform magnitudes at ≈3 Å suggests the presence of Ti−O−Zr links in the NHDG sample.

at low temperature have largely disappeared prior to crystallization. There have been several previous EXAFS and XANES studies of titanium-containing dry gels.[19,22,25−28,45,46]While Mountjoy suggested that distorted octahedral $^6$Ti was present in $(TiO_2)_x(SiO_2)_{1-x}$ xerogels,[45] with no evidence for significant amounts of $^5$Ti, Malic found five-coordinated Ti in lead titanate dry gels[28] and our previous work on CZT[19] also indicated the presence of five-coordinated titanium in the dry gels.

*Metal Ion Distributions in the Zirconate Titanate Dry Gels.* In Figure 4 the FT magnitude for a $ZrTiO_4$ dry gel sample prepared using nonhydrolytic sol−gel chemistry (NHDG) is compared with that for the $TiO_2$ dry gel sample prepared using the same processing chemistry (TNHDG). The two Fourier transforms are very different from one another, suggesting that the zirconium chloride in the reaction mixture profoundly affects the local structure of titanium in the dry gel. Both samples show peaks at ≈1−2 Å that can be attributed to backscattering from oxygen. However, the NHDG sample shows a very well-defined peak at ≈2.9 Å that is not present in the FT for the TNHDG sample. This suggests that there are significant numbers of Ti−O−Zr links in the NHDG samples. Further support for the presence of Ti−O−Zr links in the NHDG sample is provided by an examination of the back Fourier transform of the peak at ≈2.9 Å. The position of the amplitude maximum in *k*-space (subsequently referred to as $k_{max}$) is 9.3 Å$^{-1}$. However, $k_{max}$ for the metal−metal peaks in anatase and rutile were found to be at ≈8.1 Å$^{-1}$. This is consistent with the presence of zirconium in the second coordination shell of the titanium.

*Quantitative Analysis of the Ti−O EXAFS.* Four different models for the Ti−O EXAFS were tested for each of the zirconium titanate samples: (i) 4 + 2 coordination similar to the structures of anatase and rutile,[47] (ii) 2 + 2 + 2 coordination similar to the crystal structure of $CaTiO_3$, (iii) 2 + 3 + 1 coordination based on the low-temperature crystal structure of $Zr_5Ti_7O_{24}$,[5] and (iv) square pyramidal (1 + 4) coordination based on the crystal structure of $Na_2TiSiO_5$.[48] $\Delta E_0$ and $S_0$ for the analyses were fixed at the values obtained by fitting our rutile data set. Only the interatomic distances and thermal parameters ($\sigma^2$) were refined. As it was difficult to distinguish between the different six-coordinate models that were examined, only the results for 4 + 2 and 4 + 1 fits are summarized in Table 2.

**Table 2. Average Ti−O Distances Obtained by Fitting the EXAFS Data[a]**

| sample | model | $R_{av}$ (Å) | *F* value |
|---|---|---|---|
| HDG | 4 + 2 coordination | 1.90 | 11.59 |
| | 1 + 4 coordination | 1.90 | 7.98 |
| H600 | 4 + 2 coordination | 1.90 | 5.57 |
| | 1 + 4 coordination | 1.90 | 4.73 |
| H700 | 4 + 2 coordination | 1.94 | 5.78 |
| | 1 + 4 coordination | 1.94 | 15.17 |
| ADG | 4 + 2 coordination | 1.93 | 8.47 |
| | 1 + 4 coordination | 1.93 | 6.79 |
| A600 | 4 + 2 coordination | 1.91 | 10.51 |
| | 1 + 4 coordination | 1.91 | 5.86 |
| A700 | 4 + 2 coordination | 1.94 | 4.57 |
| | 1 + 4 coordination | 1.93 | 9.62 |
| NHDG | 4 + 2 coordination | 1.88 | 8.28 |
| | 1 + 4 coordination | 1.88 | 5.37 |
| NH600 | 4 + 2 coordination | 1.92 | 5.09 |
| | 1 + 4 coordination | 1.91 | 2.17 |
| NH700 | 4 + 2 coordination | 1.94 | 4.21 |
| | 1 + 4 coordination | 1.93 | 8.37 |

[a] The scale factor and $\Delta E_0$ were fixed at 0.4 and −3.31 eV, respectively. The *F* value is the sum of the squares of the differences between experimental and calculated curves and is used to describe the goodness of fit.

Model (iv) with five-coordinated Ti gave the best fit for nearly all of the amorphous samples (dry gels and 600 °C treated samples), a notable exception being the dry gel prepared using the acetic-acid-modified process (sample ADG). Regardless of which model was used, the average Ti−O distance for the amorphous materials (typically ≈1.91 Å) is shorter than that for the crystalline $ZrTiO_4$ samples. This is consistent with the titanium having an average coordination number of <6 in the amorphous materials. The crystalline $ZrTiO_4$ samples gave an average Ti−O distance of ≈1.945 Å, slightly shorter than the Ti−O distance determined by diffraction methods for the low-temperature form of $Zr_5Ti_7O_{24}$ (1.968 Å).[5] This difference may arise because diffraction methods determine the average M−O distance for a site, and in $Zr_5Ti_7O_{24}$ the cation ordering is imperfect, leading to the presence of some zirconium on the nominal titanium site. As zirconium is larger than titanium, this leads to an increase in the average M−O distance.

**Zr K-Edge EXAFS Studies.** Fourier transform magnitudes for all the Zr K-edge spectra of the $ZrTiO_4$ samples are shown in Figure 5a−c. The most pronounced differences between the samples prepared using different processing routes occur in the FT magnitudes of the amorphous materials. There are two major groups of peaks with structural significance in the FT magnitudes for all the samples, one at ≈1.6 Å (oxygen backscattering) and the other at ≈3.0 Å (metal backscattering). The peak below 1 Å that occurs in all

(45) Mountjoy, G.; Pickup, D. M.; Wallidge, G. W.; Anderson, R.; Cole, J. M.; Newport, R. J.; Smith, M. E. *Chem. Mater.* **1999**, *11*, 1253−1258.
(46) Mountjoy, G.; Pickup, D. M.; Wallidge, G. W.; Cole, J. M.; Newport, R. J.; Smith, M. E. *Chem. Phys. Lett.* **1999**, *304*, 150−154.
(47) Howard, C. J.; Sabine, T. M.; Dickson, F. *Acta Crystallogr.* **1991**, *B47*, 462−468.
(48) Nyman, H.; O'Keeffe, M. *Acta Crystallogr.* **1978**, *B34*, 905−906.

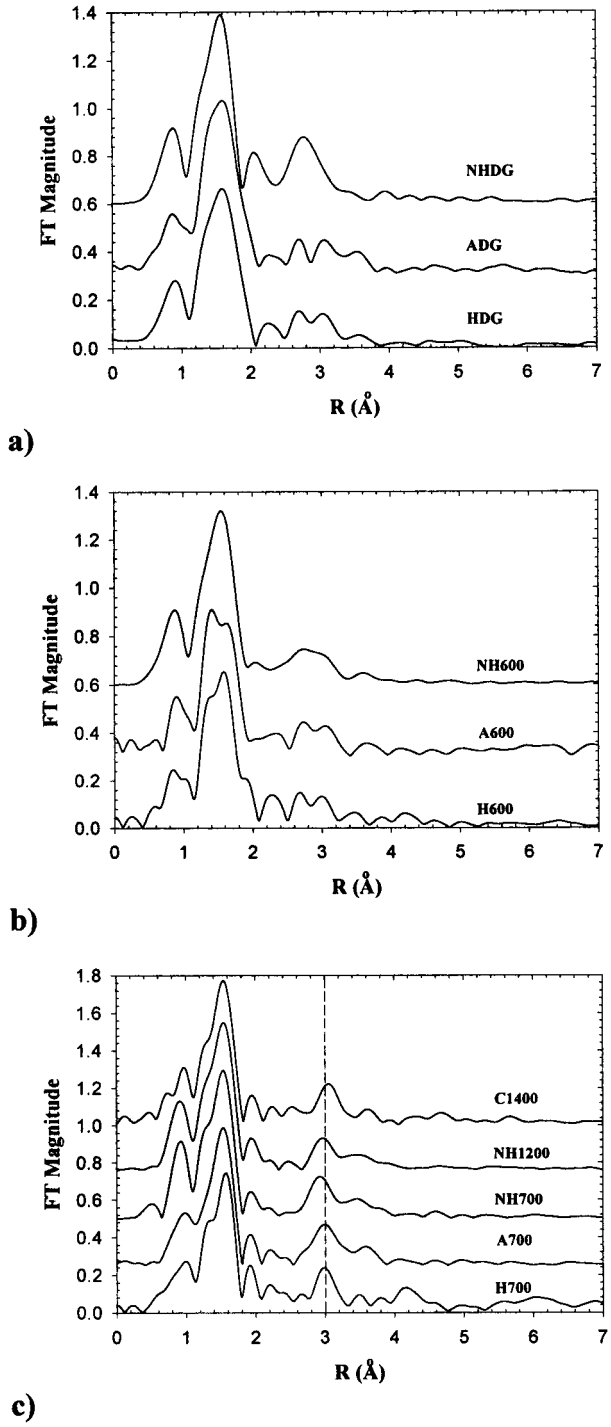


**Figure 5.** Zr K-edge Fourier transform magnitudes for all the $ZrTiO_4$ (a) dry gels, (b) samples heat-treated at 600 °C, and (c) samples heat-treated at or above 700 °C. Only the samples heated to 700 °C or more were crystalline. The Fourier transforms were carried out over the range 1−14 $Å^{-1}$. The reference line at 3.0 Å has been inserted so that it is easier to see the peak shifts that occur in this region.

the Zr K-edge FT magnitudes comes from a multielectron excitation.[49] For many of the samples there are pronounced changes in the immediate environment of the zirconium upon heating prior to crystallization. This is most obvious for the NHSG-processed samples. The peak at around ≈2.8 Å in the dry gel (NHDG) broadens and moves to longer distances upon heating to 600 °C (NH600).

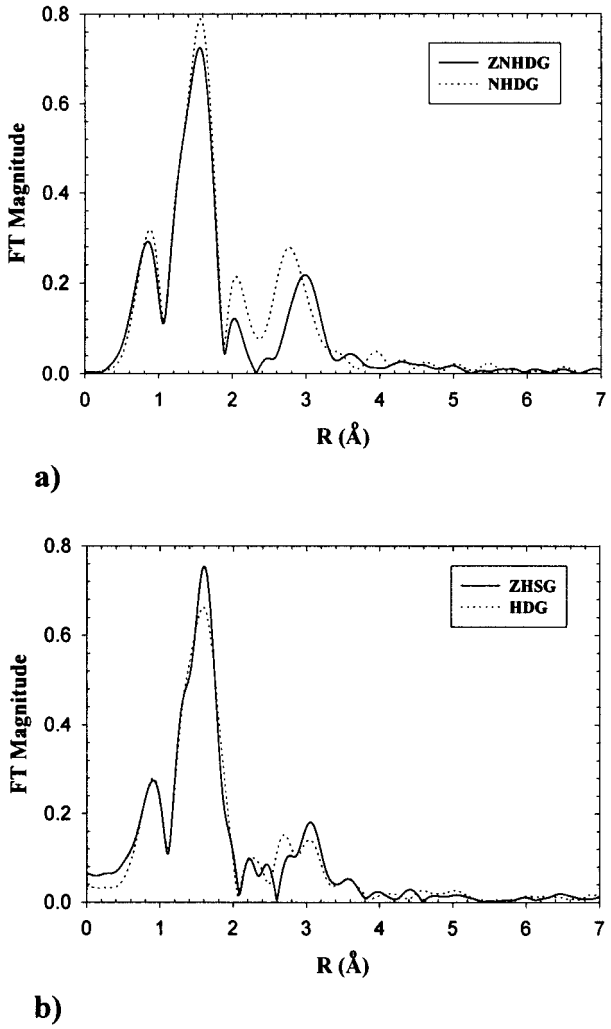


**Figure 6.** Comparisons of the Zr K-edge Fourier transform magnitudes for (a) the $ZrO_2$ (sample ZNHDG) and $ZrTiO_4$ (sample NHDG) dry gels prepared using nonhydrolytic sol−gel chemistry and (b) $ZrO_2$ (ZHSG) and a $ZrTiO_4$ (HDG) dry gels prepared by homogeneous alkoxide sol−gel chemistry.

*Zr/Ti Distribution in the Amorphous Samples.* Interestingly, the Zr K-edge FT magnitudes for the $ZrTiO_4$ (NHDG) and $ZrO_2$ ZNHDG samples (Figure 6a) prepared using nonhydrolytic sol−gel chemistry are very different from one another, even though the processing chemistry and preparation conditions used for these samples were the same other than for the presence of titanium in the $ZrTiO_4$ precursor solution. The differences are confined to the region where backscattering from neighboring metals is expected. This qualitative difference combined with the observation that the neighboring metal backscattering peak occurs at much shorter distances for the NHDG sample suggests that titanium is present in the immediate coordination environment of the zirconium in the NHDG sample. Additional evidence is provided by the back Fourier transforms of the peaks. The amplitude maxima occur at ≈8 and 10 $Å^{-1}$ for the NHDG and ZNHDG samples, respectively. This is consistent with the presence of titanium in the coordination environment of the zirconium in the NHDG sample.

(49) Wang, W.-C.; Chen, Y. *Phys. Status Solidi A* **1998**, *168*, 351−357.

A similar comparison was performed between the $ZrO_2$ (ZHSG) and $ZrTiO_4$ (HDG) dry gels prepared using alkoxide sol−gel chemistry (Figure 6b). The differences are not as pronounced as those observed for the materials prepared using nonhydrolytic sol−gel chemistry, but the FT magnitude for the HDG sample differs from that of the ZHSG sample at ≈2.8 Å. This may be indicative of the presence of Zr−O−Ti links in the HDG sample.

The issue of homo- versus heterocondensation in multicomponent sol−gel processes is of considerable interest and has been examined by a number of workers.[19,22,27,50] Unfortunately, it is often difficult to get definitive evidence on this issue. In our previous EXAFS study of solution-processed CZT,[19] we reported a possible preference for Zr−O−Zr link formation in dry gels prepared using an acetic-acid-modified route. Ahlfanger et al.[22] reported evidence for Zr−O−Ti links in PZT dry gels prepared by adding a mixture of metal *n*-propoxides (molar ratio Zr:Ti = 45:55) dissolved in the parent alcohol and acetic acid (molar ratio Ac:Zr/Ti = 1.5:1) to a stirred solution of lead acetate in methanol at 65 °C. Sengupta et al.[27] reported that Zr−O−Zr and Ti−O−Ti were the predominant links present in PZT dry gels that were prepared by mixing lead acetate, titanium isopropoxide, and zirconium *n*-propoxide in 2-methoxyethanol. Arcon et al.[50] suggested that the nature of the M−O−M links in a gel is dependent on the Zr/Ti ratio. For Zr/Ti ratios ≥1, homocondensation is more likely to take place while for Zr/Ti ratios ≤1, heterocondensation predominates. These apparently contradictory results may arise from differences in the processing chemistry that was employed.

*Zr/Ti Ordering in Crystalline $ZrTiO_4$.* The Fourier transform magnitudes for the crystalline ZT samples are compared in Figure 5c. Because the group of peaks arising from metal backscattering (at ≈3.0 Å) for these samples is quite well defined and seems to vary from sample to sample, the possibility that this variation was related to Zr/Ti ordering was explored. As mentioned earlier, the lattice constants for these samples suggest that the crystalline samples prepared at 700 °C show no Zr/Ti ordering and that the materials prepared at higher temperatures (NH1200 and C1400) are partially ordered. The FT magnitudes shown in Figure 5c do not cleanly break down into two groups and the differences that are observed do not appear to be correlated with the observed variations in the lattice constants for these materials. Currently, we do not understand the origin of the observed differences in the FTs.

*Analysis of the Zr−O EXAFS.* The Zr−O EXAFS for all of the $ZrTiO_4$ and $ZrO_2$ samples were analyzed using a single-shell model. $\Delta E_0$ and the scale factor for the analyses were obtained by fitting data for perovskite $CaZrO_3$ that were available from another series of experiments.[19] The coordination number, Debye−Waller factor, and interatomic distance were allowed to vary during the fitting of our $ZrTiO_4$ and $ZrO_2$ data. The resulting coordination numbers, interatomic distances, and Debye−Waller factors are listed in Table 3. All the crystalline $ZrTiO_4$ samples gave smaller refined coordination numbers (typically ≈4) and shorter interatomic distances (typically ≈2.07 Å) than the amorphous samples (≈5.5 and ≈2.14 Å). The refined Zr−O distances for the crystalline $ZrO_2$ samples were 2.16 Å for the monoclinic material (ZREF) and 2.18 Å for the predominantly tetragonal zirconia sample (Z600). The decrease in the Zr−O distance upon crystallization of the $ZrTiO_4$ samples (from 2.14 to 2.07 Å) strongly suggests that there is a decrease in coordination number upon crystallization. Although the absolute values of our refined coordination numbers are clearly in error, the trend that they show also indicates that the Zr coordination number is larger in the amorphous materials than in the crystalline $ZrTiO_4$ samples. The error in the absolute values of the coordination number is almost certainly related to our choice of scale factor. Using a value of 0.8 instead of 0.9 gave reasonable coordination numbers for the crystalline $ZrTiO_4$ samples, but did not change the observed trends. The measured bond lengths are consistent with the presence of six-coordinated zirconium in the crystalline $ZrTiO_4$ samples and seven-coordinated zirconium in the amorphous materials. The possibility of eight-coordinated zirconium in the crystalline $ZrTiO_4$ samples can be excluded because of the short Zr−O bond length.

**Table 3. Parameters Obtained by Fitting the Zr−O EXAFS Data[a]**

| sample | $N$ | $R_{Zr-O}$ (Å) | $\sigma^2$ (Å$^2$) | sample | $N$ | $R_{Zr-O}$ (Å) | $\sigma^2$ (Å$^2$) |
|---|---|---|---|---|---|---|---|
| HDG | 5.61 | 2.14 | 0.0085 | NH600 | 5.47 | 2.13 | 0.0083 |
| H600 | 5.30 | 2.13 | 0.0092 | NH700 | 4.18 | 2.07 | 0.0061 |
| H700 | 3.54 | 2.07 | 0.0054 | NH1200 | 4.13 | 2.07 | 0.0059 |
| ADG | 6.53 | 2.15 | 0.0091 | C1400 | 4.07 | 2.07 | 0.0063 |
| A600 | 4.39 | 2.12 | 0.0084 | ZHSG | 5.53 | 2.15 | 0.0080 |
| A700 | 3.64 | 2.06 | 0.0060 | ZNHDG | 5.69 | 2.15 | 0.0087 |
| NHDG | 5.46 | 2.13 | 0.0084 | ZNH200 | 5.60 | 2.15 | 0.0086 |

[a] $N$ is the refined coordination number. The fits were done over the range of 2−15 Å$^{-1}$. The scale factor and $\Delta E_0$ were fixed at 0.9 and −11.49 eV, respectively.

The conclusions regarding the coordination environments for the zirconium in the solution-processed samples are also supported by direct comparison of the Zr−O EXAFS for our unknowns with the EXAFS for compounds with well-defined zirconium environments. Data for monoclinic and tetragonal $ZrO_2$, $CaZrO_3$,[19] and $ZrW_2O_8$[51] were used for this comparison.

## Conclusions

The processing chemistry employed to prepare a material can, in principle, play a significant role in determining the local structure and, in particular, the compositional homogeneity of a multicomponent gel. In the case of the $ZrTiO_4$ system, if the kinetics for the formation of Zr−O−Zr, Zr−O−Ti, and Ti−O−Ti links in the gel are markedly different from one another, the compositional homogeneity that is present in an initial solution of molecular precursors may be partially lost. An inhomogeneous gel may follow a different crystallization pathway or show different crystallization kinetics from a compositionally homogeneous gel as cation diffusion over significant distances is required before the final product can be formed from an inhomogeneous gel.

(50) Arcon, I.; Malic, B.; Kodre, A.; Kosec, M. *J. Synchrotron Rad.* **1999**, *6*, 535−536.

(51) Wilkinson, A. P.; Lind, C.; Pattanaik, S. *Chem. Mater.* **1999**, *11*, 101−108.

For each of the processing routes examined, very similar crystallization behavior was observed and the local structures of the amorphous materials that were present prior to crystallization (600 °C samples) were broadly similar to one another. The titanium in each case had a coordination number of <6 and the zirconium had a coordination number >6. This suggests that the choice of processing chemistry had very little influence on the homogeneity and local structure of the calcined precursors.

While our EXAFS data for the materials prepared by alkoxide- and acetic-acid-modified methods are not completely clear on the issue of heterocondensation versus homocondensation, the data for the dry gels prepared using nonhydrolytic sol−gel chemistry strongly suggests the presence of Zr−O−Ti links. The literature contains many claims that gels produced using nonhydrolytic sol−gel chemistry are compositionally homogeneous.[52,53] However, as far as we are aware, this is the first direct evidence that a multicomponent gel produced using nonhydrolytic sol−gel chemistry is homogeneous on a short length scale.

(52) Corriu, R. J. P.; Leclercq, D. *Angew. Chem., Int. Ed. Engl.* **1996**, *35*, 1420−1436.
(53) Vioux, A.; Leclercq, D. *Heterog. Chem. Rev.* **1996**, *3*, 65−73.

**Acknowledgment.** This work was primarily supported by a NSF award, DMR-9623890. The authors gratefully acknowledge the use of beamline X-11A at the National Synchrotron Light Source, Brookhaven National Laboratory. X11A is supported, in part, by the U.S. Department of Energy, Division of Materials Science under Contract DE-FG02-89ER45384. We are indebted to Dr. Ingrid Pickering for assistance with the EXAFS data collection at SSRL. The EXAFS facilities at the Standford Synchrotron Radiation Laboratory are operated as part of the SSRL Biotechnology Program, which is supported by the National Institutes of Health, National Center for Research resources, Biomedical Technology Program, and by the Department of Energy, Office of Biological and Environmental Research.

**Supporting Information Available:** Powder X-ray diffraction patterns for the heat-treated $ZrO_2$ and $TiO_2$ samples prepared using nonhydrolytic sol−gel chemistry and conventional alkoxide chemistry as well as tables of the observed lattice constants for the crystalline $ZrTiO_4$ samples and the positions and heights of the major peaks in each of the Ti K pre-edge spectra. This material is available free of charge via the Internet at http://pubs.acs.org.

CM000298S